

# The University of Tokyo Atacama 1.0-m Telescope

Takeo Minezaki<sup>a</sup>, Daisuke Kato<sup>b</sup>, Shigeyuki Sako<sup>a</sup>, Masahiro Konishi<sup>a</sup>, Shintaro Koshida<sup>a</sup>, Natsuko Mitani<sup>a</sup>, Tsutomu Aoki<sup>c</sup>, Mamoru Doi<sup>a</sup>, Toshihiro Handa<sup>a</sup>, Yoshifusa Ita<sup>d</sup>, Kimiaki Kawara<sup>a</sup>, Kotaro Kohno<sup>a</sup>, Takashi Miyata<sup>a</sup>, Kentaro Motohara<sup>a</sup>, Takao Soyano<sup>c</sup>, Toshihiko Tanabé<sup>a</sup>, Masuo Tanaka<sup>a</sup>, Ken'ichi Tarusawa<sup>c</sup>, Yuzuru Yoshii<sup>a</sup>, Leonardo Bronfman<sup>e</sup>, Maria T. Ruiz<sup>e</sup>, and Mario Hamuy<sup>e</sup>

<sup>a</sup>Institute of Astronomy, University of Tokyo, Tokyo, Japan;

<sup>b</sup>Institute of Space and Astronomical Science, Japan Aerospace Exploration Agency, Sagamihara, Japan;

<sup>c</sup>Kiso Observatory, University of Tokyo, Kiso, Japan;

<sup>d</sup>Department of Astronomy, Tohoku University, Sendai, Japan;

<sup>e</sup>Department of Astronomy, University of Chile, Santiago, Chile

## ABSTRACT

We present the current status of the University of Tokyo Atacama 1.0-m telescope constructed at the summit of Co. Chajnantor (5,640 m) in Atacama, Chile, which is an optical/infrared telescope at the world's highest site. The telescope is an f/12 Ritchey-Chretien type with a field of view of 10 arcmin. It is installed in a 6-m dome and is controlled from the operation room in a container separated from the dome. The engineering first light observation was carried out in March 2009, and the astronomical observations have been carried out since June 2009. The pointing of the telescope is as accurate as 2.4 arcsec (RMS), showing good tracking accuracy of 0.2 arcsec for 60-s observation without guiding. The Hartmann constant is 0.19 arcsec and the image quality of the telescope is satisfactory for scientific observations. The best PSF obtained is 0.5 arcsec (FWHM) in optical, which demonstrates that the summit of Co. Chajnantor is one of the best seeing site in the world. Also the excellent atmospheric transmission in infrared wavelength at the site is proved by successful observations carried out by the ANIR near-infrared camera and the MAX38 mid-infrared instrument. In the near future, the operation room will be connected to the base support facility at San Pedro de Atacama for remote observation.

**Keywords:** telescope, near infrared, mid infrared, Atacama, high altitude, remote observation, Co. Chajnantor

## 1. INTRODUCTION

The University of Tokyo is currently planning to construct a 6.5-m telescope optimized for the infrared observations at the summit of Cerro (Co.) Chajnantor (5,640 m) in Atacama, Chile, called the University of Tokyo Atacama Observatory (TAO) project (PI: Yuzuru Yoshii),<sup>1</sup> and the University of Tokyo Atacama 1.0-m telescope is a prior project of the 6.5-m telescope.<sup>2</sup> The construction of the 1.0-m telescope at the summit of Co. Chajnantor is started in the end of 2008, and the engineering first light observation was carried out in March 2009. The ANIR near-infrared camera<sup>3</sup> and the MAX38 mid-infrared instrument<sup>4</sup> can be equipped on the Cassegrain focus, and scientific observations for various targets have been carried out since June 2009. It is now an optical/infrared telescope at the world highest site, and unique results are expected by infrared observations with low background and high sensitivity through newly-opened atmospheric windows. In Section 2, the site of Co. Chajnantor will be described. The 1.0-m telescope and support facilities will be described in Section 3, and the performance of the telescope will be reported in Section 4. In Section 5, the future plan of remote operation will be described.

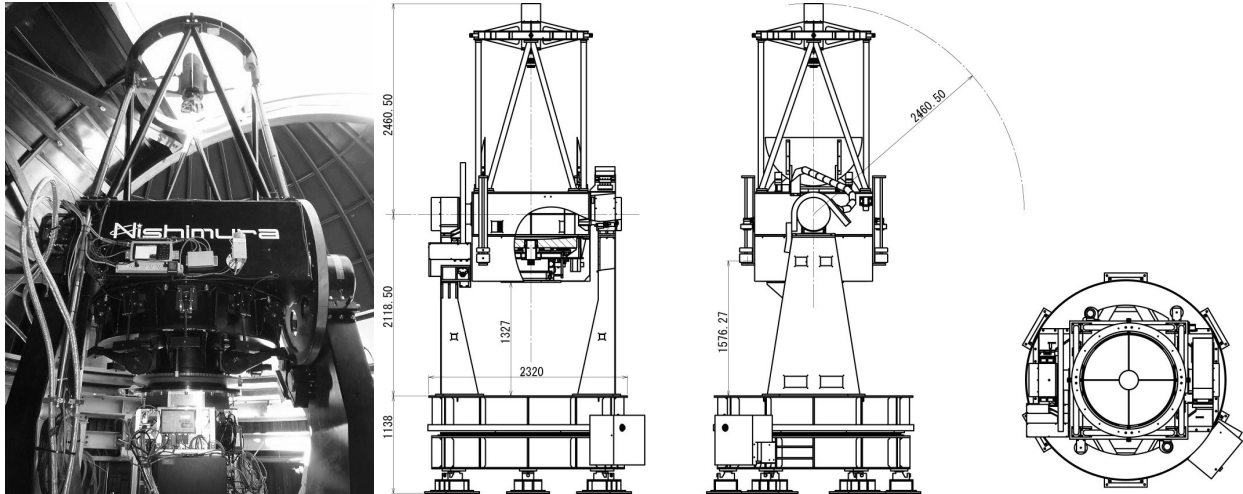


Figure 1. The University of Tokyo Atacama 1.0-m telescope installed in the 6.0-m dome at the summit of Co. Chajnantor, and its schematic illustrations.

## 2. SITE

The Atacama Desert is one of the driest regions on the Earth, located in northern Chile. On the eastern side of the desert, the Chajnantor plateau and the Pampa La Bola plateau over 5,000 m altitude extend, which are widely known to be one of the best site for radio astronomy. Seeking for stable and high-transparent atmospheric environment, a number of radio telescopes, including the Atacama Large Millimeter/Submillimeter Array (ALMA), have been constructed.

Co. Chajnantor is a peak at an altitude of 5,640 m, lying between the Pampa La Bola plateau and the Chajnantor plateau. Because of the high altitude and the dry condition, the precipitable water vapor (PWV) at Co. Chajnantor is very low, 0.4 to 1.3 mm based on the satellite data analysis,<sup>5</sup> which is much lower than that at the Mauna Kea observatory (0.9 to 2.8 mm). According to the model calculation of the atmosphere, new atmospheric windows in mid-infrared wavelength beyond 30  $\mu\text{m}$  will appear, and also the absorption bands in the near-infrared wavelength at 0.8 to 2.5  $\mu\text{m}$  will become transparent at the summit of Co. Chajnantor. Indeed, successful observations carried out by ANIR<sup>6</sup> and MAX38<sup>7</sup> proved those newly-opened atmospheric windows. The seeing condition at the summit is comparable or even better than most of the major observatories. The best seeing of 0.38 arcsec and the median seeing of 0.69 arcsec in optical were measured by the differential image motion monitor (DIMM) observation carried out for 8 nights during 2006 to 2007.<sup>8</sup> Weather and cloud cover at the summit are also monitored for years, showing that fraction of clear nights is over 90 % except winter season.<sup>9</sup> These results demonstrate that the summit of Co. Chajnantor is one of the best sites for the infrared astronomy on the Earth.

## 3. TELESCOPE AND FACILITIES

### 3.1 Overview of the telescope

The University of Tokyo Atacama 1.0-m telescope is a standard reflecting telescope on an alt-azimuth mount, and is optimized for infrared observations. Figure 1 shows a photograph and schematics of the telescope, and Table 1 summarizes the telescope specifications. The telescope optics is a Ritchey-Chretien type reflector with a clear aperture of 1042 mm, and the final focal ratio is 12.0. Only the Cassegrain focus is available, and the field of view is 10 arcmin in diameter. Reduction of thermal emission from the telescope structure is crucial for infrared observations. Therefore, a light baffle, which becomes a source of background emission in infrared, is omitted from the telescope optics. An oversized primary mirror (1060 mm in diameter) is employed and a center cone is placed on the secondary mirror to avoid thermal emission from outside the primary mirror and the Cassegrain hole. In addition, spider cover mirrors are attached on the bottom face of the spider arms to reduce

Table 1. Specifications of the telescope.

Optical system		Cassegrain/Ritchey-Chretien
Primary mirror	Clear Aperture	1042.4 mm
	Focal Ratio	2.5
Secondary mirror	Size	222.88 mm
	Radius of Curvature	-1407.673 mm
Final Focal Ratio		12.0
Back Focus		650.0 mm
Field of View		$\phi 10$ arcmin
Plate Scale		16.644 arcsec mm <sup>-1</sup>
Max. Rotation Speed	Azimuth	3 deg s <sup>-1</sup>
	Elevation	2 deg s <sup>-1</sup>
	Rotator	3 deg s <sup>-1</sup>
Max. Dimension of an Instrument		$\phi 1000$ mm $\times$ 1150 mm
Max. Loading Capacity on the Focus		300 kg

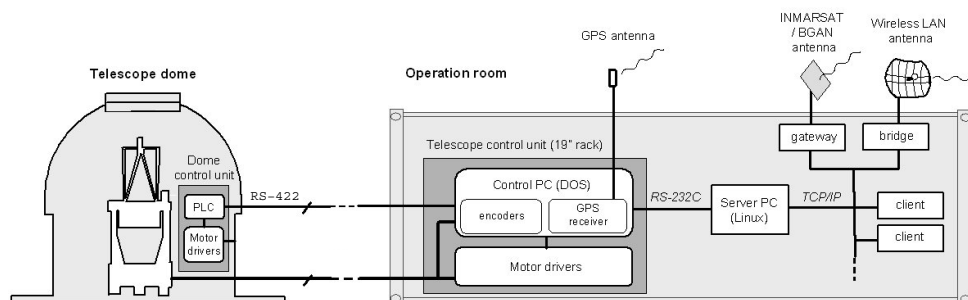


Figure 2. The schematic diagram of control system for the telescope. The telescope and the dome are managed with a DOS-based control PC installed in the operation room. Users control the telescope and the dome via a Linux-based server PC. The summit network is connected to Internet via the INMARSAT/BGAN satellite communication, and a wireless LAN bridge that links the summit network and the base support facility is planned.

emissions from the spider arms themselves and surrounding structures reflected on surfaces of the spider arms coming into the Cassegrain focus.

The structure of the telescope is designed and fabricated by Nishimura Co. Ltd. The primary mirror is housed in a mirror cell and is mounted by three fixed points and the 18-points whiffletree support with 10 side pads, balancing its loads by counter weights. The azimuth (Az-) and elevation (El-) rotation axes are driven by friction drives with servo motors, at the maximum speeds of 3 deg s<sup>-1</sup> and 2 deg s<sup>-1</sup>, respectively. The R-guide arc-shaped bearing systems (THK Co., LTD), which were first employed for the IRSF 1.4-m telescope by Nishimura Co. Ltd., are mounted between the azimuth rotation disk and the base disk as the bearing of the Az-axis to make the size of the telescope compact. An instrument rotator is installed on the Cassegrain focus, and it can be driven at the maximum speeds of 3 deg s<sup>-1</sup>. The maximum dimension of an instrument attached on the focus is  $\phi 1000$  mm  $\times$  1150 mm, and the maximum loading capacity on the focus is 300 kg. To minimize the external noise coming into the instruments caused by the driving motor of the telescope, line filters are inserted in the power lines of the motors and the motor drivers, and we find no additional noise for ANIR and MAX38.



Figure 3. A full view of the summit facilities. From right to left, the telescope dome, the operation container, the storage container, and the generator container are seen.

Figure 2 shows a schematic diagram of the control system of the telescope and the dome. A DOS-based control PC in the operation room, which is synchronized with GPS time, controls both the telescope and the dome. A dome control unit consisting of motor drivers and programmable logic controllers (PLCs) in the dome, which is managed by the control PC in the operation room through a RS-422 interface, drives the dome azimuth rotation and the dome slit. A TCP/IP socket server running on a Linux-based PC accepts control commands from client softwares, then translate them into low-level commands and send them to the control PC through a RS-232C interface. In addition to the client softwares that are used for the normal operation of the telescope and dome, a handset unit is available for the basic operation.

### 3.2 Summit and Base Support Facilities

Figure 3 shows a full view of the summit facilities. A 6-m dome, three containers and solar panels were constructed at the summit of Co. Chajnantor. The dome, in which the telescope is installed, is located on the southwest ridge of the summit, the windward side, to obtain better seeing.<sup>9</sup> Schematics of the 6-m dome are shown in Figure 4. The primary mirror of the telescope is installed at a height of 3.5 m from the ground. Observation instruments are carried into the Cassegrain floor from an entrance at the second floor. An 8-m container next to the dome is used for an operation room at the summit, and the telescope, the dome, and the observation instruments are controlled from this operation container. Another two 20-ft containers are installed for a storage and a power generator. A diesel generator of 125 kVA capacity supplies sufficient power for observations even in low-oxygen environment. A solar power system of 1.1 kW capacity supplies power to a minimum portion of the network system, monitoring cameras, and weather monitor systems, when the generator does not work. The LAN of the summit facilities is connected to Internet via the INMARSAT/BGAN satellite communication, whose maximum data rate is 0.5 Mbps.

A base support facility with an office room and a storage is now under construction at San Pedro de Atacama, the nearest town located at 48 km to the west of the summit, at an altitude of ~2400 m. In the near future, the base facility will be directly connected to the summit for remote operation from the base facility, as will described in Section 5.

### 3.3 Site Construction

Before the site work started, in June 2008, the telescope was assembled in the factory of the telescope vendor in Japan to carry out a test operation. Both ANIR and MAX38 were mounted on the telescope to examine

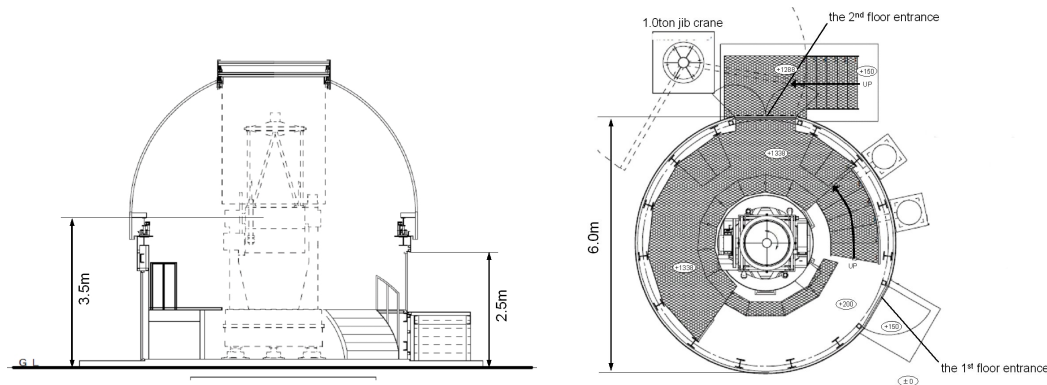


Figure 4. Schematics of the 6-m dome. (left) Cross-sectional elevation view from the first floor entrance. (right) Cross-sectional plane view. Up side is north. The 6m dome and the summit facilities are constructed by Kokusai Kogyo Co. Ltd and Nishimura Co. , Ltd.

the interface on the focus, the electrical noise from the telescope driving motors, and the operation with the telescope. The telescope was disassembled and shipped to Chile in November 2008.

The site work at the summit of Co. Chajnantor started with the groundwork of the telescope and buildings in the end of 2008. In parallel with the site work at the summit, the telescope was assembled again at a factory space at Calama, the nearest city located about 100 km away from San Pedro de Atacama, in February to March. We carried out a test operation again and confirmed that the telescope worked well even after the long transportation. After the test operation, the telescope was again disassembled into several large components to be transported to the summit of Co. Chajnantor. The installation of the telescope into the 6-m dome started on March 12. Finally, on March 22, 2009, the engineering first light observation was carried out by a CCD camera attached on the Cassegrain focus of the telescope.

After the engineering first light observation, the telescope control system in the dome and the operation container were completed in June 2009, and the telescope became able to be controlled from the operation container. We also continued to improve the telescope performances, which will be reported in the next section. Now, the telescope and dome are ready for scientific observations. The first scientific observation was carried out by ANIR, on June 9, 2009, and the first scientific observation by MAX38 was carried out on November 8, 2009.

## 4. PERFORMANCE EVALUATION

### 4.1 Pointing Accuracy

The pointing accuracy of several arcseconds is required to minimize the field-of-view overlap in large area imaging surveys. The telescope analysis was carried out to model the alignment errors of the telescope structure, which increase pointing errors, then they were corrected by software to improve the telescope pointing. The misalignment and flexure of the telescope are expressed with the following parameters in the pointing model: (1) an offset of a zero-point for the Az- and El- encoders; (2) a tilt for the Az-axis against the zenith; (3) non-perpendicularity of the Az-axis relative to the El-axis; (4) nonperpendicularity of the optical axis to the El-axis; (5) flexure of the optical support structure; and (6) a precession of the Az-axis, which is supposed to be caused by alignment errors of the R-guides mounted on the base disk. The observation for the telescope analysis was carried out by an SBIG ST-8XME CCD camera attached on the telescope, whose pixel scale and field of view were  $0.15 \text{ arcsec pixel}^{-1}$  and  $3.8 \times 2.5 \text{ arcmin}^2$ , respectively. We targeted  $\sim 100$  stars distributed uniformly over the sky and measured their pointing errors, that is the angular separations between the target positions and the image center of the CCD. The pointing model was calculated from the sky positions of the targeted stars and their pointing errors using the TPOINT software (provided by P. T. Wallace). The pointing errors along the Az- and El-axes after the correction of the pointing model are presented in the left panel of Figure 5. The pointing accuracy of the telescope, which is estimated by a root mean square (RMS) of the pointing errors for  $\sim 100$  stars over the whole sky, reaches 2.4 arcsec after several iterations of the telescope analysis.

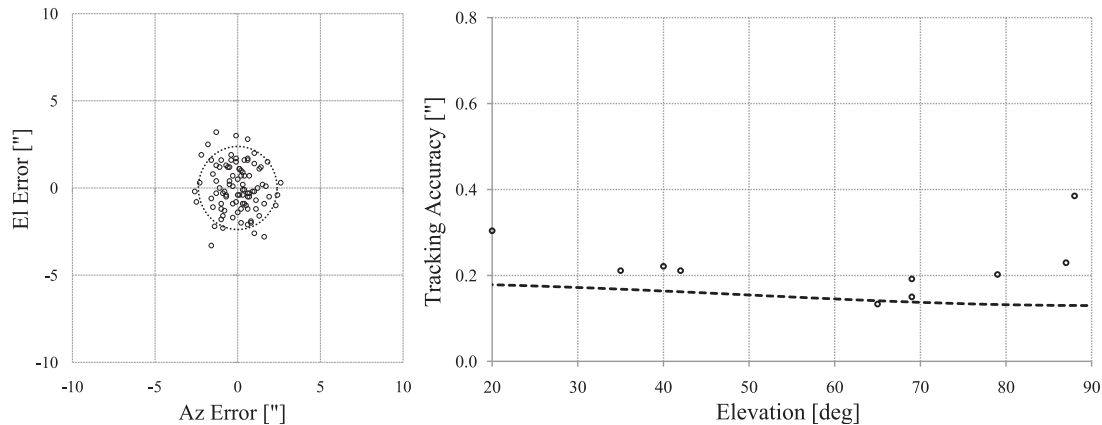


Figure 5. (*left*) The pointing errors along the Az- and El-axes for  $\sim 100$  stars over the whole sky. Dashed circle represents the RMS of the pointing errors of 2.4 arcsec in radius. (*right*) The measured tracking accuracy. The dashed line represents the tracking error expected from the driving accuracies of the Az- and El-axes. Units of elevation and tracking accuracy are degree and arcsec, respectively.

## 4.2 Tracking Accuracy

The tracking accuracy of 0.2 arcsec, which corresponds to the best seeing (FWHM  $\sim 0.4$  arcsec) at the summit of Co. Chajnantor, is required to avoid image blurring. Since the driving errors of the Az- and El-axes is directly linked to the tracking errors, we first examined the driving accuracy. The Az- and El-axes of the telescope were driven with a constant speed of  $15 \text{ arcsec s}^{-1}$ , and the differences between directed positions calculated by the telescope controller and actual positions indicated by the encoder were recorded in every 0.1 s during 90-s driving. The driving accuracy was estimated by calculating an RMS of the differences, at the positions in every  $10^\circ$  of both axes, corresponding to 36 positions for the Az-axis and seven positions for the El-axis ( $20^\circ$ – $80^\circ$ ). We found that the driving accuracy is 0.13 arcsec on average in both axes.

Next, we examined the tracking accuracy by tracking a star and measuring its drift motion. A bright star was monitored for 300 s by a WATEC WAT-100N video CCD camera attached on the telescope, then its position on the CCD was calculated in every 1 s. An RMS of the deviation of the position was calculated for every 60 s, and the tracking errors for each observation was estimated by averaging five measurements of the RMS deviation. We carried out 10 sets of observations in different elevations. The tracking errors we measured are presented in the right panel of Figure 5. Although the tracking errors at the highest and lowest elevations are larger, most of them are as small as about 0.2 arcsec, which enables us to obtain images without losing original quality limited by seeing at the summit. The tracking accuracy is estimated at 0.21 arcsec for 60-s observation, by averaging the tracking errors except that at  $88^\circ$  in elevation.

The dashed line in the same figure represents the tracking error expected from the driving accuracies of 0.13 arcsec in the Az- and El-axes. The measured tracking errors almost follow the expectation from the driving accuracies, except at the highest and lowest elevations. At around the zenith, the Az- and rotator axes of an alt-azimuth mount moves so fast that the pointing correction values change quickly, even during a few-minutes tracking. Therefore, the tracking error becomes sensitive to the accuracy of the pointing model at highest elevations, then the large tracking error of 0.39 arcsec at  $88^\circ$  in elevation is supposed to be caused by small errors in the pointing model. On the other hand, the image motion of a star caused by atmospheric turbulence becomes large in low elevations with an increase in airmass. The measurement of the tracking accuracy at  $20^\circ$  in elevation showing large value of 0.30 arcsec could be affected by atmospheric turbulence.

## 4.3 Optical Performance

The optical performance of the telescope was evaluated by the Hartmann test carried out on October 4, 2009. A Hartmann plate with circular holes, whose diameter was 25 mm, and which were located in a rectangular pattern with a pitch of 100 mm, was mounted on the top ring. Then, a pair of defocused images at the

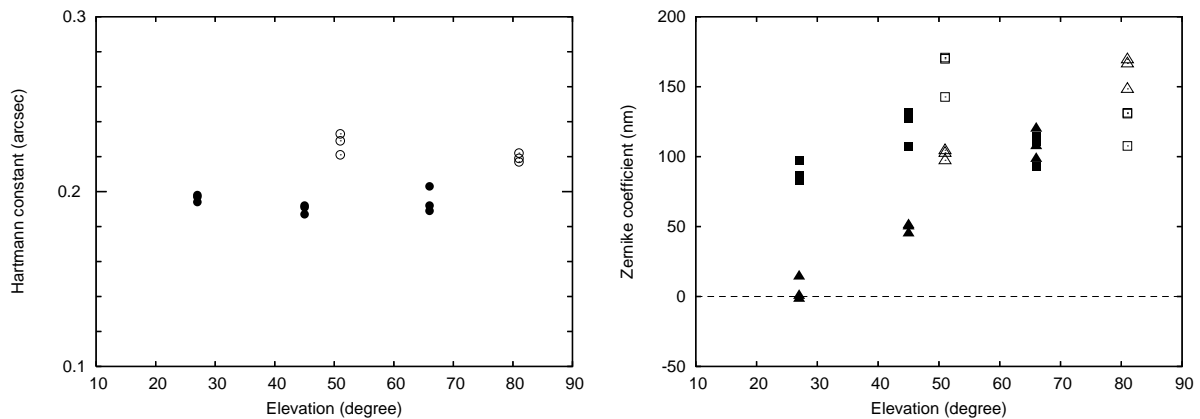


Figure 6. The results of the Hartmann test. (left) The Hartmann constants. The open circles represent the measurements of the first two sets of observations, and filled circles represent those of the later three sets of observations. (right) The wavefront aberration decomposed by the Zernike polynomials. The squares represent the Zernike coefficient of astigmatism, and the triangles represent that of trefoil astigmatism. The open marks represent the measurements of the first two sets of observations, and filled marks represent those of the later three sets of observations.

secondary-mirror positions of  $\pm 4$  mm shifted from the best focus was obtained by the ST-8 CCD camera. We used 63 Hartmann spots in the defocused image to calculate a Hartmann constant and analyze wavefront errors. Five sets of observations, including three measurements for each set, were carried out in different elevations. The best-focus position was gradually changed with time during the first two sets of observations, which suggests that the telescope temperature was not settled to ambient one. Therefore, the data of the first two sets could be affected by the dome and mirror seeing and/or small flexure of the telescope structures caused by inhomogeneous temperature distribution.

The Hartmann constants we measured are presented in the left panel of Figure 6. Although those of the first two sets of observation (open circles) are slightly larger, those of the later three sets (filled circles) agree with each other, at about 0.19 arcsec, and show no dependence on elevation. The Hartmann constant of 0.19 arcsec corresponds to 0.36 arcsec in FWHM, estimated by fitting a Gaussian radial profile to the encircled energy profile derived from the spot diagram of the Hartmann test. It is comparable to the best seeing of 0.38 arcsec and much smaller than the median seeing of 0.69 arcsec measured by the DIMM observation. These results show that the telescope has good optical performance over the whole sky.

The wavefront aberration was analyzed by fitting the Zernike polynomials to the wavefront error derived from the Hartmann test, and we found that astigmatism and trefoil astigmatism showed large contribution to the wavefront error. The Zernike coefficients of the astigmatism (open and filled squares) and trefoil astigmatism (open and filled triangles) are presented in the right panel of Figure 6. The astigmatism of the wavefront error shows no dependence on elevation, which is supposed to be caused by small misalignment between the primary and the secondary mirrors or that of the primary mirror support system. On the other hand, the trefoil astigmatism of the wavefront error increases clearly with elevation, which is supposed to be caused by small adjustment errors of the counterbalancing weight of the primary mirror support.

Figure 7 shows a sample image obtained by the ST-8 CCD camera and the radial profile of a star in the image. The best PSF obtained during the engineering observation was about 0.5 arcsec in FWHM, which proves that the performance of the telescope optics and the tracking accuracy is satisfactory for scientific observations. In addition, assuming that the FWHM of PSF observed by the CCD camera equals to a square-root of square sum of the seeing FWHM and the PSF FWHM of the telescope optics, the best PSF obtained corresponds to the seeing FWHM of about 0.36 arcsec, which agree with the best seeing measured by the DIMM observation. We also note that the PSF FWHMs of 0.5 – 0.6 arcsec were not at all rare during the engineering observation, even though air conditioning system to improve the dome and mirror seeing is not installed in the dome, and

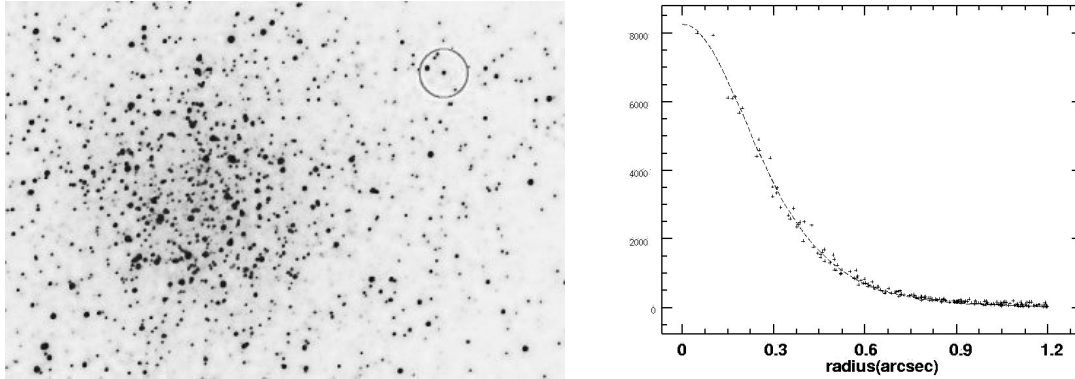


Figure 7. The best PSF obtained during the engineering observation. (left) A sample image of a globular cluster, 47 Tucanae, obtained by the ST-8 CCD camera with an exposure time of 30 sec in the red filter. (right) The radial profile of a star circled in the left panel. The FWHM is measured at about 0.5 arcsec.

the primary mirror is placed only 3.5 m high from the ground, which might be insufficient to avoid the ground layer turbulence. These results indicate that the summit of Co. Chajnantor is one of the best seeing site in the world.

## 5. REMOTE OPERATION

The atmospheric pressure at the summit of Co. Chajnantor is only a half of that of sea level, and the air temperature drops down to about  $-10^{\circ}\text{C}$ . In these severe environments, the operation at the summit is physically demanding. In addition, time for observation is restricted by duration of a portable oxygen tank used for oxygen inhalation at the summit, which is required to avoid the risk of hypoxia. Therefore, we are planning to operate the telescope, the dome and the instruments from the base facility, to carry out scientific observations. The remote operation will reduce the physical load and increase the observing efficiency.

The INMARSAT/BGAN satellite communication currently available is inadequate for the remote operation because of its large latency and expected cost. Then, new network system is planned, which is designed by Ubiteq, Inc. The summit facility will be linked with the base facility by two pairs of 2.4 GHz wireless LAN bridges, one is active and the other is backup. The transfer rate is expected to increase to a few Mbps, and the latency will be negligible. After the direct link is connected, the satellite communication will be used as another backup line.

Extensive monitoring system is crucial for remote observation. A high-sensitivity video camera is mounted on the operation container to monitor the dome, and another high-sensitivity camera is mounted on the center section of the telescope to monitor the dome slit and the night sky viewed by the telescope. A total of seven monitoring cameras, which can record sound with video, are placed in the dome and the containers. A weather monitor terminal and an all-sky infrared cloud monitor are mounted on the operation container. All these monitoring data are automatically stored in the database system, and can be access via web-based interface to facilitate the remote operation.

All the equipments at the summit should be prepared for power failure or other kind of troubles. Most equipments except power-consuming ones are supported by UPSs. When the diesel generator suspends unexpectedly, the dome slit automatically closes. In addition, a minimum portion of the summit network and the monitoring system will be supplied with power from the solar system to monitor the status of the summit facilities during power outage.

## ACKNOWLEDGMENTS

We thank all the workers at Monte Grande Co. at Calama, Chile for construction of the summit facilities and the access road, and Kokusai Kogyo Co. , Ltd. and Andes Co. , Ltd for the arrangements of our activities in Chile.



We are grateful to all of the members of Nishimura Co. , Ltd for their supports in telescope tests. We also thank Nano-Optonics Research Institute for helpful support. This work has been supported by the Grants-in-Aid for Scientific Research (15253001, 17104002, 20041003, 21018003, and 21018005) from the JSPS. Part of this work has been also supported by NAOJ Research Grant for Universities, and by the Advanced Technology Center, NAOJ.

## REFERENCES

- [1] Yoshii, Y. et al., “The University of Tokyo Atacama Observatory 6.5m telescope project,” *Proc. SPIE*, in this conference (2010).
- [2] Sako, S. et al., “The University of Tokyo Atacama 1.0-m telescope,” *Proc. SPIE* **7012**, 70122T–70122T–10 (2008).
- [3] Motohara, K. et al., “ANIR: Atacama near infrared camera for Paschen  $\alpha$  imaging,” *Proc. SPIE* **7014**, 70142T–70142T–10 (2008).
- [4] Miyata, T. et al., “A new mid-infrared camera for ground-based 30 micron observations: MAX38,” *Proc. SPIE* **7014**, 701428–701428–8 (2008).
- [5] Erasmus, F. S. and van Staden, C. A., “A satellite survey of cloud cover and water vapor in northern Chile,” A study conducted for Cerro Tololo Inter–American Observatory and University of Tokyo (2001).
- [6] Motohara, K. et al., “First Paschen  $\alpha$  imaging from the ground: the first light of Atacama Near-Infrared Camera on the miniTAO 1m telescope,” *Proc. SPIE*, in this conference (2010).
- [7] Nakamura, T. et al., “MiniTAO/MAX38 first light: 30-micron band observations from the ground-based telescope,” *Proc. SPIE*, in this conference (2010).
- [8] Motohara, K. et al., “Seeing environment at a 5640m altitude of Co. Chajnantor in northern Chile,” *Proc. SPIE* **7012**, 701244–701244–10 (2008).
- [9] Miyata, T. et al., “Site evaluations of the summit of Co. Chajnantor for infrared observations,” *Proc. SPIE* **7012**, 701243–701243–8 (2008).